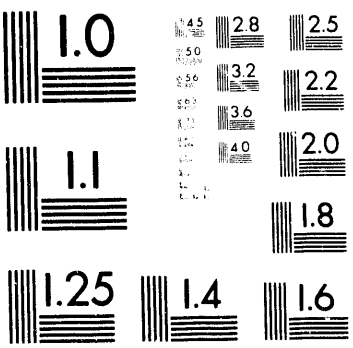
1.0
2.8
2.5
3.2
2.2
3.6
2.0
4.0
1.1
1.8
1.25
1.4
1.6

1 of 1

CONF-9309130--1
SAND--93-1881C

Magnetic Force Microscopy/Current Contrast Imaging: A New Technique for Internal Current Probing of ICs

Ann N. Campbell, Edward I. Cole, Jr., Bruce A. Dodd, and Richard E. Anderson

Department 2275, Failure Analysis, Electronics Quality/Reliability Center, Sandia National Laboratories, Albuquerque, NM 87185

This invited paper describes recently reported work on the application of magnetic force microscopy (MFM) to image currents in IC conductors [1]. A computer model for MFM imaging of IC currents and experimental results demonstrating the ability to determine current direction and magnitude with a resolution of ~ 1 mA dc and ~ 1 μA ac are presented. The physics of MFM signal generation and applications to current imaging and measurement are described.

1. INTRODUCTION

Performing detailed integrated circuit (IC) analysis requires the measurement of internal conductor voltage and current during operation. While highly developed techniques for voltage measurement on IC conductors have been available for some time, at present there is no practical technique for determining IC currents. The ability to detect current magnitude and direction is highly desirable for design verification, analysis of analog circuits in which currents convey information, and analysis of failures whose only signature is anomalous current with no other detectable attribute. Previously, asymmetric secondary electron emission around current-carrying conductors in a scanning electron microscope (SEM) was used to detect 100 mA ac currents on IC test structures [2]. However, the utility of this approach is limited because of low sensitivity and voltage contrast effects. In the present work we describe a new technique for non-invasive imaging of currents in operating ICs based on scanning probe microscopy (SPM).

An obvious signature of charge flow in a conductor is the resulting "cylindrical" magnetic field about the conductor (Ampere's Law) [3]. The technique offering the best sensitivity and spatial resolution for detection of the magnetic field associated with currents in operating ICs is magnetic force microscopy (MFM). The MFM technique has been used as a sensitive probe to image magnetic fields and domains in magnetic thin films [4-7] with spatial resolution approaching 10 nm [8]. In this paper we describe the first application of MFM to detection of current in operating ICs. We demonstrate the feasibility of using the MFM current contrast imaging (MFM/CCI) technique to image currents in operating ICs and show that this technique can detect the magnitude and direction of dc current and the magnitude and phase of ac current.

MASTER
DISTRIBUTION OF THIS DOCUMENT IS UNLIMITED

2. BACKGROUND: PRINCIPLES OF MAGNETIC FORCE MICROSCOPY

Magnetic force microscopy is one of a growing family of scanning probe microscopy techniques. Samples are imaged in an SPM by scanning a sharp probe tip attached to a cantilever in close proximity to the sample surface [9,10]. There are two operating modes, contact and non-contact. MFM is a non-contact SPM technique.

In non-contact mode (also known as attractive mode) SPM, the tip is moved 10 to 100 nm away from the sample surface [9]. Some spatial resolution is lost in non-contact mode relative to contact mode because the tip is at a greater distance from the sample surface. Long range interactions (i.e., Van der Waals, magnetic, and electrostatic) dominate the interaction between the tip and sample in non-contact mode imaging. The sensor (tip) must be capable of interacting with the field of interest. In the absence of other field gradients, the tip is attracted to the sample surface by Van der Waals forces, which may be used to generate a topographic image of the surface. Magnetic field gradients may be imaged by MFM when the tip has a sufficient magnetic dipole moment. Depending upon the relative strength of the magnetic field and Van der Waals gradients as well as the characteristics of the magnetic tip, the non-contact mode image may show only the magnetic field effects, a superposition of magnetic and topographic effects, or only topography. Forces resulting from electric fields were not significant compared to magnetic and Van der Waals forces in our experiments.

In non-contact mode SPM, the tip is vibrated perpendicular to the sample surface with sufficient amplitude (~ 1 nm) to prevent it from being drawn into contact with the surface by the attractive forces. Tip vibration is achieved by oscillating the cantilever supporting the tip at or near its resonance frequency. The local field gradients parallel to the direction of tip vibration (dF_z/dz) interact with the vibrating tip and modify the effective spring constant, C, of the cantilever according to $C = C_0 + dF_z/dz$, where C_0 is the spring constant of the isolated cantilever [9]. If the interaction is attractive, the cantilever effectively softens (i.e., its spring constant decreases), with the result that the resonance frequency also decreases. Conversely, a repulsive interaction leads to an increase in the resonance frequency. Changes in the interaction force may be detected by monitoring the amplitude, phase, or frequency of the cantilever's vibration.

3. APPROACH

3.1 Simulation of MFM Current Contrast Imaging

A simple computer model was developed to assess the feasibility of using MFM to image current in operating ICs. The model was used to calculate the magnetic fields produced by different currents in several parallel, straight conductors and to simulate the MFM image for the given conditions. The conductors were assumed to be infinitely thin, infinitely long, and spaced 5 μm apart. The local magnetization was assumed to be zero (0) and the permeability of free space was used for all modeling. The magnetic field around the four parallel conductors in the model is the superposition of the fields generated around each one.

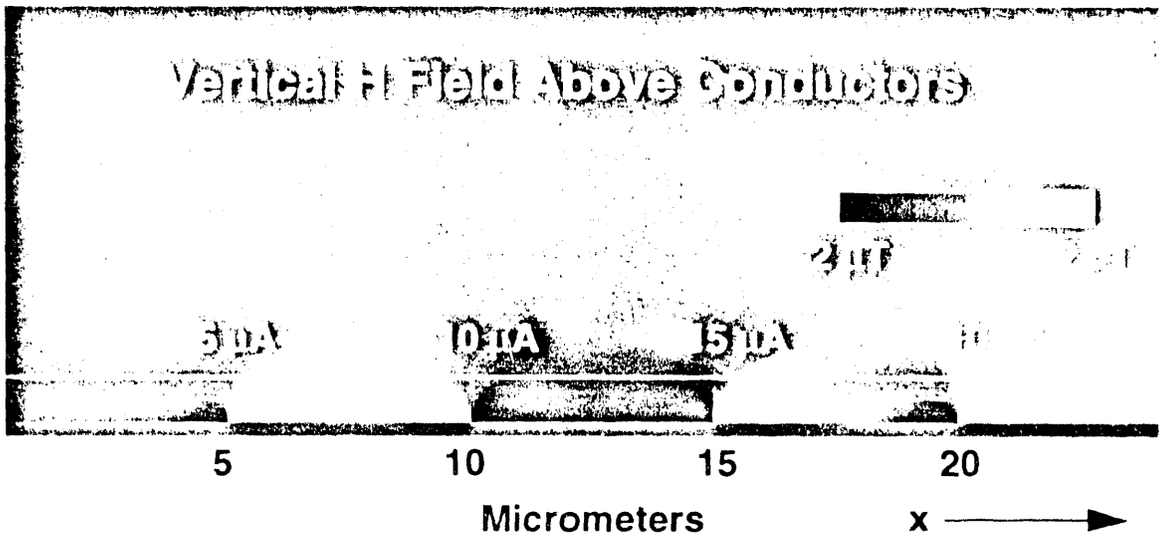

Figure 1. Simulation of vertical magnetic field component, H_z, above four parallel current-carrying conductors.

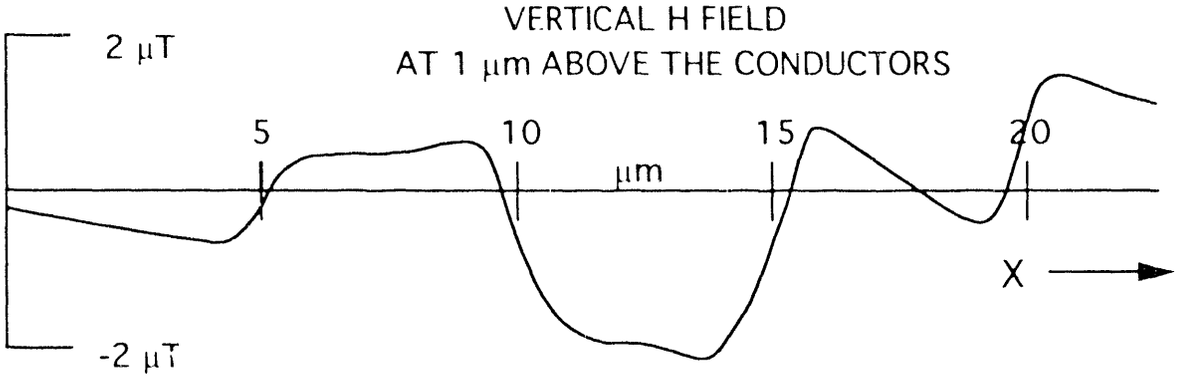

Figure 2. Simulation of an MFM linescan 1 μm above the conductors shown in Fig. 1.

Figure 1 shows a cross-section through the conductors with the magnitude and direction of the dc current through each indicated. The background contrast indicates the vertical component of the magnetic field, H_z, above the conductors. As discussed in the Section 2, H_z is the component of the magnetic field to which the MFM is most sensitive. Figure 2 is a linescan showing the variation of H_z with position (x) at a height of 1 μm above the conductors. Because of the passivation layer on ICs, the MFM tip will typically be at least 1 μm above the conductors. The model does not include an attenuation factor for the passivation because it does not appreciably reduce the magnetic field intensity. The magnetic field strengths are on the order of microtesla (μT) for the simulated currents. Figure 3 shows the simulated MFM image of an isolated, straight conductor with 2 mA dc current. Beginning at the bottom of the figure, the dc current was initially - 2 mA. The bright-to-dark transition (from left to right) occurs because H_z changes sign above the conductors as indicated in the linescan in Figure 2. The y-axis in Figure 3 indicates both distance along the conductor and time of the raster scan. When the current direction was reversed (from -2 mA to + 2 mA as indicated in Figure 3), the bright-to-dark contrast in the simulated image was also reversed.

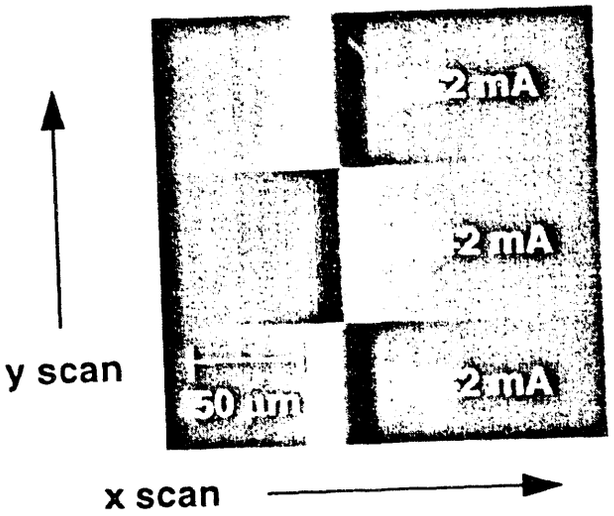

Figure 3. Simulated MFM image of a conductor carrying 2 mA dc current.

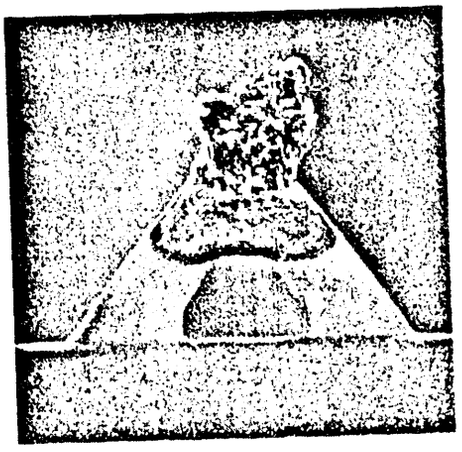

Figure 4. MFM tip fabricated by attaching a NdFeB filing to a micromachined cantilever.

Three-dimensional simulations using actual IC conductor geometries have been performed [11, 12] based on the theory of Hartmann [13]. Our results are in good agreement with those of the 3-dimensional models at a distance of 1 μm (passivation thickness) from the conductor.

3.2 Experimental Implementation of MFM for Current Contrast Imaging

3.2.1 Non-Contact Mode Imaging

A Park Scientific Instruments SFM-BD2 scanning probe microscope with a non-contact mode detection module was used to acquire MFM data and images. The frequency modulation (FM) non-contact mode technique was employed. The system automatically determines and locks in on the resonance frequency of the cantilever. The vibration amplitude of the cantilever is held constant, and changes in its vibration frequency as the tip interacts with magnetic fields on the sample are detected. The operating frequency is shifted away from the resonance frequency by an amount proportional to the desired interaction force between the tip and magnetic fields on the sample. The frequency shifts are detected by a phase detector, and the difference between the selected operating frequency and the cantilever's natural resonance frequency is referred to as the phase acceptance window. A feedback circuit adjusts the tip-sample spacing to maintain a constant force on the tip as the sample is scanned.

3.2.2 Magnetic Tips

The characteristics of the magnetic tip are of great importance to the system response. Our best results to date were achieved by using cyanoacrylate to attach filings of a neodymium-iron-boron (NdFeB) magnet to commercially-available, micromachined Si_3N_4 cantilevers. While this approach yields tips with sufficient magnetic dipole moment to detect and image currents in operating ICs, our control over tip geometry is limited and the dipole direction must be determined by experiment. One of the magnetic tips used in this study is shown in Figure 4. The magnet is large and irregular in shape, which limits the spatial resolution of our measurements.

There are important differences between the sensors required for MFM imaging of magnetic recording media and those needed for IC current contrast imaging. A tip with a small magnetic dipole moment is required for imaging recording media because a strong magnetic sensor could distort the data being read [14]. Tips with small moments are sufficient because the fields being sensed are relatively strong. In MFM current contrast imaging of ICs, the magnetic field is weaker and a sensor with a larger magnetic dipole moment is required. In this case, the sample has no permanent magnetic properties which could be altered by a sensor with a relatively large magnetic dipole moment.

3.2.3 DC and AC Stimulation

MFM current contrast images were obtained with both dc and ac stimulus. DC stimulus gives rise to static magnetic field gradients around the conductor, which are detected readily by attractive mode imaging. It is also possible to detect ac currents by taking advantage of the mechanics of the vibrating cantilever, which can be represented as a simple harmonic oscillator. When ac stimulus is applied to an IC, the magnetic field and field gradients vary with the frequency of the applied signal, ω_1. The vibration amplitude, A, of a simple harmonic oscillator with external force applied can be expressed as $A \propto 1/(\omega_0^2 - \omega_1^2)$ where ω_0 is the cantilever resonance frequency [15]. As the ω_1 approaches ω_0, the amplitude of vibration increases rapidly. In practice, this means that the sensitivity of the system increases dramatically if the ac signal is applied to the conductor at ω_0.

3.2.4 MFM Signal Acquisition.

A schematic of the MFM acquisition system used at Sandia National Laboratories is shown in Figure 5. The main console controls the fine mechanical approach, the piezoelectric scanning (x, y, and z) of the sample, the piezoelectric bimorph that vibrates the cantilever at resonance, the reference frequency, and the phase acceptance window. A reference frequency between 60 kHz and 270 kHz may be selected on our MFM system. Because of their relatively large mass, the cantilevers produced at Sandia National Laboratories have a resonance frequency of ~22 kHz. Fortunately, the system is capable of sensing harmonics of the resonance frequency, so a reference frequency of ~66 kHz was used. Both the cantilever's resonance frequency and the user selected reference frequency are displayed on an oscilloscope.

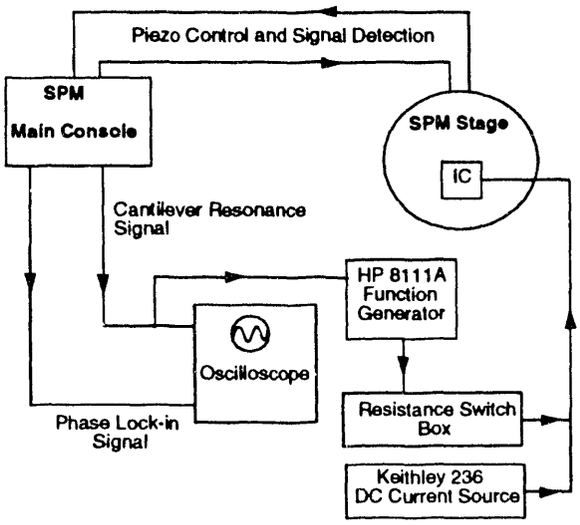

Figure 5. Schematic of the MFM acquisition system.

Electrical stimulation was performed with both dc and ac current. A variable resistance switch box was used to select the ac current through the IC. The cantilever's resonance signal was used to trigger a function generator to insure synchronization with the cantilever's resonance frequency for ac

experiments. Because the sample stage rather than the tip is scanned in our system, it was necessary to avoid restricting the motion of the sample stage with multiple electrical connections from the bias source to the sample. Our approach was to connect only two conductors to the IC package on the SPM stage. Electrical connection was made from these two pins to all the necessary pins on the IC by wire bonding.

The placement of the cantilever close to the IC surface proved to be a difficult mechanical problem. Figure 6 shows how the SPM test head holding the Pyrex base of the cantilever is positioned in the IC package cavity above the IC die. Cantilever deflection is sensed with a reflected laser beam. The coarse positioning is performed by mechanically lowering the SPM test head into the package well. Note that the SPM test head must be at an angle to clear the sides of the IC package cavity. Figure 7 is a higher magnification view of the cantilever approaching the sample. The micromachined cantilever and its tip are much smaller than the Pyrex base attached to the SPM test head.

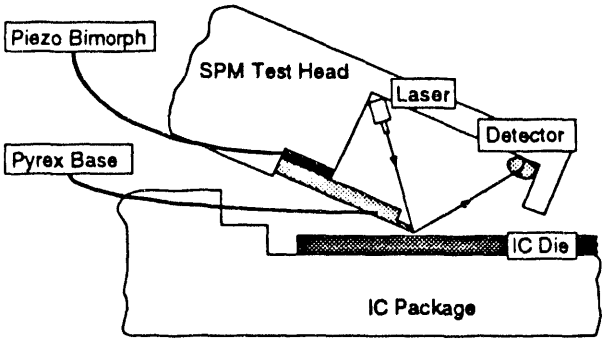

Figure 6. The SPM test head in position to acquire data from a packaged IC.

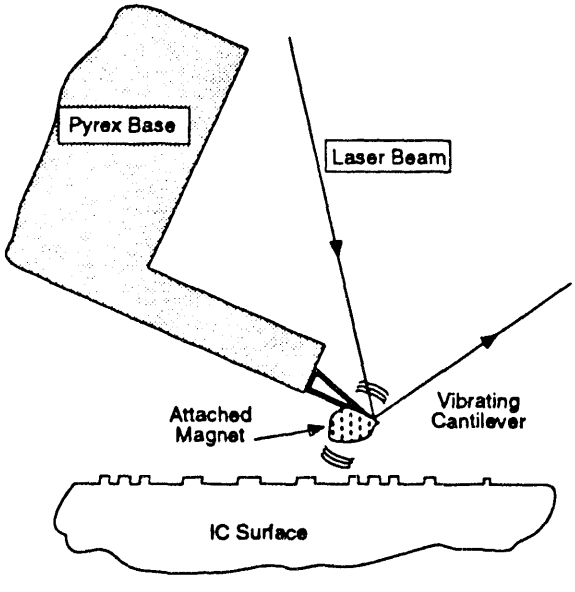

Figure 7. The vibrating cantilever interacts with fields near the IC surface.

4. MFM IMAGING AND MEASUREMENT RESULTS

4.1 DC Analysis

Figure 8 is an optical micrograph of the test structure used for dc and ac analysis. The two aluminum conductors shown are 4 μm wide. Current is passed through the conductor on the right. The conductor on the left is electrically floating for all measurements and images. For optimal signal and spatial resolution the gain of the z-piezoelectric drive was maximized and the scan speed minimized. The high gain of the z-piezoelectric feedback maximized the SPM's response (and hence signal) to the forces encountered while scanning. The slow scan speed (15 minutes/image) ensured that the SPM could respond to magnetic forces encountered during the raster scan before the cantilever had moved away from the source of those forces.

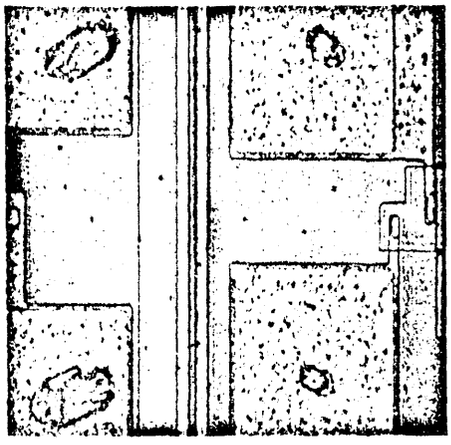

Figure 8. Optical micrograph of passivated test structure used for dc and ac analysis. The two conductors run vertically between the four bond pads.

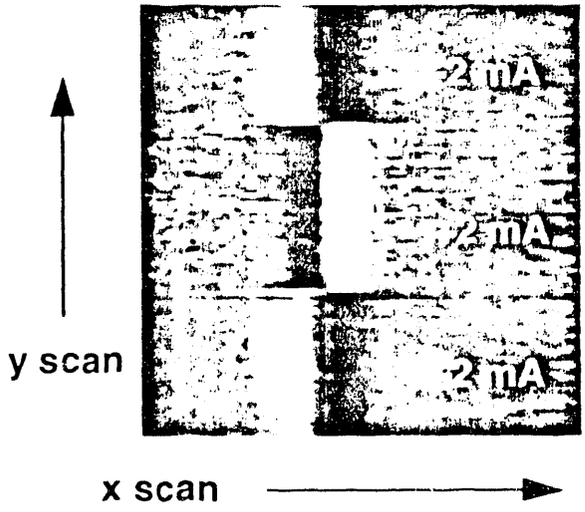

Figure 9. MFM image of the test structure in Figure 8 with ± 2 mA dc current applied during the raster scan.

Figure 9 is an MFM image of the passivated test structure shown in Figure 8 with ± 2 mA dc current in the conductor. The current was initially - 2 mA, and the corresponding MFM image is the bottom third of Figure 9. The current direction was changed during acquisition of the image. The middle section of the image displays the vertical magnetic field gradients when the applied current is + 2 mA, and at the top of the image the current is again - 2 mA. The conductor is located at the bright/dark-dark/bright interface in the middle of the image. Note that this is very similar to the modeled MFM image shown in Figure 3.

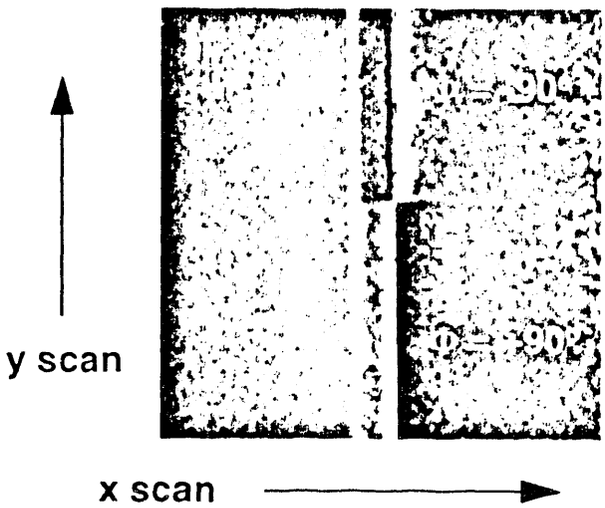

Figure 10. MFM image of the test structure with 20 μA ac current applied during the raster scan.

Images similar to Figure 9 were obtained for applied dc currents of ± 500 μA and ± 250 μA [1]. As indicated in Section 3.2.3, the MFM signal decreases as the applied current drops. For applied dc currents of < ± 250 μA, the signal was lost in the noise.

4.2 AC Analysis

AC square wave currents were also analyzed using the test structure shown in Figure 8. As discussed in Section 3.2.3, large increases in current (magnetic field) sensitivity can be achieved by changing the current through the conductor at the resonance frequency of the cantilever. Figure 10 shows the MFM signal of a 20 μA

peak-to-peak current through the conductor. Halfway through acquisition of the image the phase of the ac current was changed by 180^{0}, causing the bright/dark signal to shift sides of the conductor. The increase in sensitivity was so great that smaller magnetic tips with a reduced net magnetic dipole moment (not usable for dc measurement) were adequate for ac analysis as shown here. The use of a physically smaller tip increased the spatial resolution to the point that the topology of the unbiased conductor on the left is now visible as a Van der Waals force image superimposed on the magnetic field image.

4.3 Current Sensitivity of MFM/CCI

By "parking" the MFM cantilever close (~10 μm) laterally to one side of the conductor and monitoring the change in MFM signal with applied current, the sensitivity of the MFM to differences in applied current can be demonstrated. Figure 11 shows a plot of normalized MFM signal response to applied dc current. Zero (0) MFM signal at zero (0) current has been added as a data point in Figure 11 with no error bars. These data indicate that a change of ~ 1 mA over the ± 5 mA range is easily detected. A "best-fit", 3rd order polynomial fit to the data is displayed in Figure 11. The exact shape of the curve depends upon the effect of external force gradients on the cantilever's resonance properties as well as the MFM system's response over the signal range.

Figure 12 shows the MFM signal response to ac currents. These data were also acquired by "parking" the cantilever and acquiring the MFM response versus applied ac current. The straight line fit of the data in Figure 12 indicates that shifts of ~1 μA can be detected over this 20 μA peak-to-peak ac range.

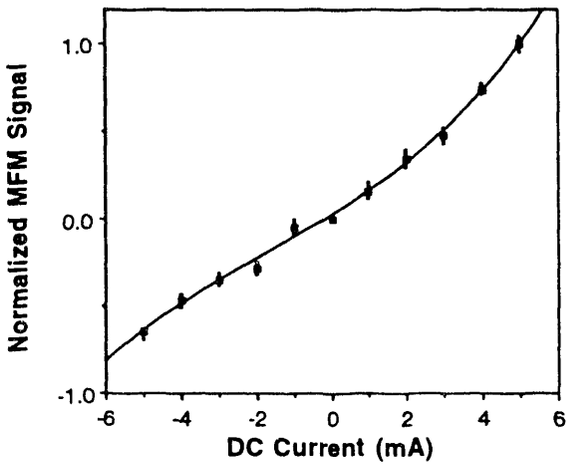

Figure 11. Plot of normalized MFM signal as a function of applied dc current.

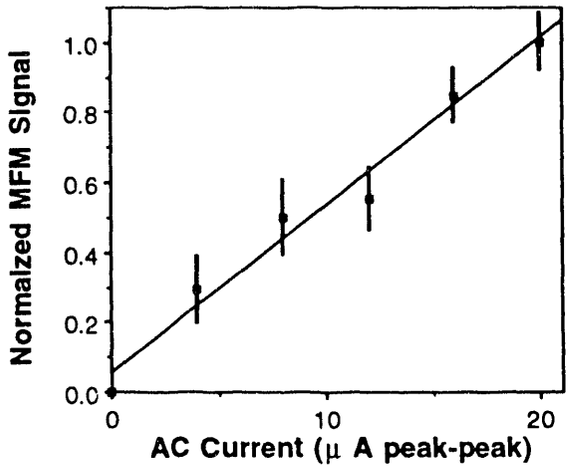

Figure 12. Plot of normalized MFM signal as a function of applied ac current.

Note that Figures 11 and 12 *do not* indicate that currents can arbitrarily be measured to within 1 mA dc or 1 μA ac, but *do show* that *changes* in current magnitude as low as 1 mA dc

and 1 μA peak-to-peak ac can be detected. The lateral "parking" distance from the conductor, the vertical distance above the DUT surface, the reference frequency and phase acceptance window, as well as the particular cantilever used all contribute to the MFM's response to different currents (magnetic fields). Further work to standardize these variables will be necessary to make accurate, quantitative current measurements.

4.4 Application of MFM/CCI to a Defective IC

A damaged IC with elevated power supply current was examined with MFM/CCI. The IC has two levels of metal interconnect (1.25 μm metal-1 and 1.75 μm metal-2). A metal-1 to metal-2 short was produced by using a laser to fuse a metal-2 signal conductor to a metal-1 V_{DD} power bus. The IC drew 10 mA dc current with 3.3 V applied bias. Most of this current was a result of the laser damage since the IC current level was < 50 μA at 5 V before fusing.

Figure 13 is a dc MFM/CCI image of the elevated current path on the damaged IC. The bright/dark interface that runs horizontally from the lower left to center and then vertically indicates the conductor location. Figure 14 is an optical micrograph of approximately the same field of view as Figure 13, with the current-carrying conductors highlighted in white. Even though the current path is a backwards "L" in shape as shown in Figures 13 and 14, the conductor actually has a "T" shape; the conductor forming the vertical part of the current path continues to the bottom of the image. Electrical continuity was confirmed at this interconnection using voltage contrast imaging. This demonstrates that the actual current path can be determined by MFM/CCI from among multiple possible paths.

The same IC was also examined using ac current with similar results. The power supply used to bias the IC had a dc voltage of 3.225 with a superimposed ac ripple of 0.075 V. This concept of applying a "ripple" to the IC's power supply has been introduced for I_{DDQ} testing with no adverse effects on the IC [16,17]. The results of these measurements are discussed further in Reference 1.

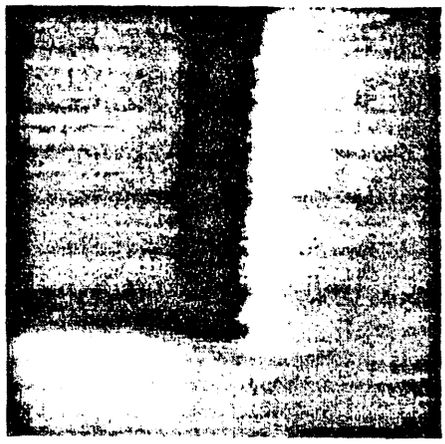

Figure 13. MFM current contrast image of the elevated current path on a damaged IC. Conductor location coincides with the bright/dark transition.

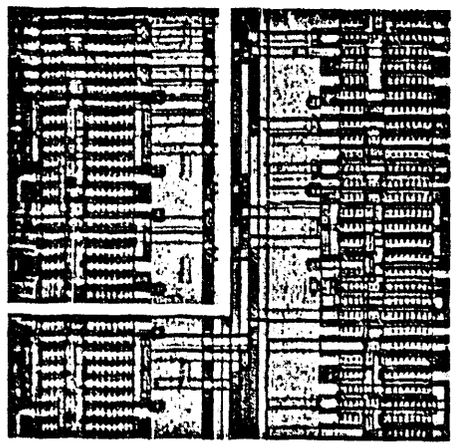

Figure 14. Optical micrograph of the same field of view as Figure 13, with the current path highlighted in white.

The dc and ac MFM/CCI images shown in Figures 9, 10, and 13 were obtained from passivated structures. However, no differences in spatial or current resolution were observed when repeating the experiments with the passivation removed. This is probably a result of the very large magnetic tip used compared to the passivation thickness.

5. DISCUSSION

While we have demonstrated that magnetic force microscopy can be used to image dc and ac current in packaged test structures and ICs, further development of the technique will be required for it to become a standard failure analysis tool. First, the capability to scan and image an entire IC, rather than a small area (250 x 250 μm), is mandatory. Second, a fully-developed system must be able to accommodate both packaged ICs and wafers and allow for electrical stimulus. Third, a manufacturable technique for producing magnetic tips with well-controlled magnetic properties must be established. In addition, development of an MFM/CCI capability for quantitative current waveform analysis would be a desirable enhancement to the tool.

Some of the necessary improvements in SPM technology are already being made by the commercial SPM manufacturers. Most notably, systems with large-area scanning capability are becoming available. These systems feature a large mechanical translation stage which is typically designed to accommodate an 8" wafer. The probe tip and piezo scanners are mounted above the stage, which translates the sample so that the desired area may be imaged. Such a system could be easily modified to accommodate packaged ICs and fixturing so that MFM data could be collected while the IC is being tested. A large-area image could be developed by taking a series of scans and mosaicking the images, but this could be very time consuming. Large area mechanical scanning in the x- and y-directions may offer a better solution. By contrast, the system we have used to develop MFM/CCI is an "older generation" system in which the piezoelectric scanners drive the sample rather than the probe tip. Because the piezo scanners are fragile, this severely limits the mass of the sample that can be imaged. Further, the physical design of the microscope limits the size of the sample that can be accommodated.

The manufacture of magnetic tips requires major development before MFM examination of ICs can become routine. The design of the magnetic tips must be optimized for both magnetic field sensitivity and spatial resolution; in general, small tips which are capable of high spatial resolution have a correspondingly small magnetic dipole moment. Our crude process of attaching a magnetic filing to the end of a micromachined cantilever had a low yield of "usable" tips (about 1 our of 15). We had no method of determining the suitability of a fabricated tip prior to testing it in the MFM system. Methods to control tip variables such as orientation of magnetic field, magnetic coercivity, magnetization, net magnetic dipole moment, as well as physical dimensions must be developed. MFM tips made by sputter-coating standard micromachined cantilevers with a magnetic material (typically a cobalt-chromium (CoCr) alloy [14]) are becoming commercially available. Our preliminary evaluation is that these tips may not have sufficient magnetic dipole moment for dc MFM/CCI analysis, but that they will probably be useful in ac analysis. Certainly further work with

various materials and fabrication techniques is required to achieve uniform, reproducible, well-characterized tips for MFM analysis of IC currents.

While ac analysis has been shown to greatly increase the current sensitivity, it has also proved to be too sensitive in some cases. Future work to "desensitize" the MFM system by operating slightly out of phase with the cantilever's resonance frequency would permit ac analysis with a larger dynamic range.

6. CONCLUSIONS

We have demonstrated the ability to image internal IC currents non-invasively for the first time. The magnetic fields associated with current-carrying conductors were imaged by the MFM/CCI technique. MFM current contrast imaging with sensitivities of 1 mA dc and 1 μA ac is an important new capability for failure analysis and design verification. Both current and voltage imaging of internal conductors on operating ICs are now feasible by combining the current contrast imaging technique demonstrated here with conventional electron-beam voltage contrast techniques which have been highly developed in recent years.

These results indicate the great potential of applying MFM to IC failure analysis and are indicative of the growing importance of scanning probe microscopy in this field. However, the MFM current contrast technique is very much in its infancy. Considerable development work will be required to make MFM/CCI a standard failure analysis tool.

ACKNOWLEDGMENTS

The authors thank Park Scientific Instruments for technical assistance with attractive mode imaging, R. Proksch and E. Dan Dahlberg of the University of Minnesota for supplying magnetic thin-film coated tips and unpublished modeling results, J. M. Soden and C. L. Henderson for critical review of the manuscript, and the Sandia National Laboratories Laboratory Directed Research and Development (LDRD) Office for support of this work. This work was performed at Sandia National Laboratories and supported by the U. S. Department of Energy under contract number DE-AC04-76DP00789.

REFERENCES

1. A. N. Campbell, E. I. Cole, Jr., B. A. Dodd, and R. E. Anderson, 31st Annual Proceedings of the International Reliability Physics Symposium (1993) 168.
2. K. Helmreich, P. Nagel, W. Wolz, K. D. Muller-Glaser, Proceedings of the International Test Conference (1991) 256.
3. D. Halliday and R. Resnick, Physics, John Wiley & Sons, Inc., New York, 844 - 846, 1966.
4. Y. Martin and H. K. Wickramasinghe, Appl. Phys. Lett., 50 (1987) 1455.
5. Y. Martin, D. Rugar, and H. K. Wickramasinghe, Appl. Phys. Lett., 52 (1988) 244.

6. H. J. Mamin, D. Rugar, J. E. Stern, B. D. Terris, and S. E. Lambert, Appl. Phys. Lett., 53 (1988) 1563.
7. P. C. D. Hobbs, D. W. Abraham, and H. K. Wickramasinghe, Appl. Phys. Lett., 55 (1989) 2357.
8. P. Grutter, Th. Jung, H. Heinzelmann, A. Wadas, E. Meyer, H.-R. Hidber, and H.-J. Guntherodt, J. .Appl. Phys., 67 (1990) 1437.
9. D. Rugar and P. Hansma, Physics Today, (October 1990) 23.
10. H. K. Wickramasinghe, Scientific American, (October 1989) 98.
11. R. Proksch, unpublished results.
12. T. Goddenhenreich, H. Lemke, M. Muck, U. Hartmann, and C. Heiden, Appl. Phys. Lett., 57 (1990) 2612.
13. U. Hartmann, J. Vac. Sci. .Technol. A, 8 (1990) 411.
14. P. Grutter, D. Rugar, H. J. Mamin, G. Castillo, S. E. Lambert, C.-J. Lin, R. M. Valletta, O. Wolter, T. Bayer, and J. Greschner, Appl. Phys. Lett., 57 (1990) 1820.
15. H. Goldstein, Classical Mechanics, 2nd ed., Addison-Wesley, Reading, MA, 264 - 265, 1980.
16. M. W. Levi, Proceedings of the IEEE Test Conference, (1981) 217.
17. J. M. Soden, C. F. Hawkins, R. K. Gulati, and W. Mao, J. of Electronic Testing, 3 (1992) 291.

DISCLAIMER

This report was prepared as an account of work sponsored by an agency of the United States Government. Neither the United States Government nor any agency thereof, nor any of their employees, makes any warranty, express or implied, or assumes any legal liability or responsibility for the accuracy, completeness, or usefulness of any information, apparatus, product, or process disclosed, or represents that its use would not infringe privately owned rights. Reference herein to any specific commercial product, process, or service by trade name, trademark, manufacturer, or otherwise does not necessarily constitute or imply its endorsement, recommendation, or favoring by the United States Government or any agency thereof. The views and opinions of authors expressed herein do not necessarily state or reflect those of the United States Government or any agency thereof.

DATE
FILMED
11/15/93

END